IEEE Access
Multidisciplinary | Rapid Review | Open Access Journal

Received January 8, 2018, accepted January 20, 2018, date of publication February 21, 2018, date of current version March 12, 2018.

Digital Object Identifier 10.1109/ACCESS.2018.2805281

In-Situ Observations of Lithium Dendrite Growth

LINGXI KONG, YINJIAO XING, AND MICHAEL G. PECHT, (Fellow, IEEE)
Center for Advanced Life Cycle Engineering, University of Maryland, College Park, MD 20742 USA

Corresponding author: Michael G. Pecht (pecht@calce.umd.edu)

This work was supported by the Center for Advanced Life Cycle Engineering.

ABSTRACT One of the root causes of lithium battery failure is lithium dendrite formation. Dendrites can result in internal short circuits and ultimately thermal runaway, fires, and explosions. Unfortunately, it has been difficult to study dendrites due to an inability to conduct in-situ observations. This paper presents an *in-situ* observation approach, consisting of an optically transparent lithium battery cell to observe dendrite growth evolution while concurrently monitoring the electrical characteristics of the cell under various current densities.

INDEX TERMS Dendrite growth, internal short circuit, current density, in-situ observation.

I. INTRODUCTION

Safety is a significant concern in electronic products powered by lithium-ion batteries, in spite of technological improvements in lithium-ion battery chemistry and design [1], [2]. One cause of thermal runaway, fires and explosions is lithium dendrites [3], [4]. A lithium dendrite is a metallic microstructure that is formed on the anode and will grow toward the cathode, typically during the battery charging process. Once the dendrite connects two electrodes, it will enable the current to pass through, thus heating the surrounding organic materials and triggering an exothermic reaction, often leading to thermal runaway [5], [6].

The investigation of dendrites is challenging because their evolution is the result of a combination of different factors, including electrolyte composition [7]–[10], ambient temperature [11]–[13], and current density [14]–[18]. The joint effects of these factors is expected to cause different lithium dendrite growth rates and morphologies.

Electrolyte composition is expected to have a significant impact on dendrite formation because it affects the composition of the solid electrolyte interphase (SEI) layer where dendrites initiate. Jeong *et al.* [7] found the SEI formed in propylene carbonate (PC) electrolyte with higher $LiN(SO_2C_2F_5)_2$ concentrations can retard dendrite growth and improve the cycling efficiency. Liu *et al.* [19] showed their co-doped electrolyte can delay dendrite growth compared with several other composite solid polymer electrolytes. Mogi *et al.* [20] tested the dendrite blocking effect of PC-based electrolyte with different organic additives. They found that electrolyte with fluoroethylene carbonate (FEC) improved the battery life of the sample with the lithium-metal anode.

In terms of temperature dependencies on dendrite growth, Love *et al.* [11] studied dendrite growth on symmetric Li cells in the electrolyte of EC:DMC (ethylene carbonate and dimethyl carbonate) with 1 M $LiPF_6$ at three temperatures (−10, 5, and 20 °C). All the three samples were charged using a constant current of 5 mA/cm^2. They observed dendrites having a mushroom-shaped structure at −10°C and a needle-like shape at 5 °C and 20 °C. Aryanfar *et al.* [21] conducted constant charging tests on symmetric Li cells in the electrolyte of PC with 1 M $LiClO_4$ at 21, 48, and 70 °C, respectively. Comparing the average dendrite lengths from all the three samples tested using a constant charge current of 2 mA/cm^2, they observed that dendrite grew more slowly at higher temperatures. They attributed this phenomenon to a thermal relaxation effect, which facilitates the diffusion of lithium atoms diffuse from the protruding part to flat section. Akolkar [12] also mathematically modeled dendrite growth. The model-based simulation provides an estimate of the dendrite growth rate ratio, which is defined as the ratio of the localized current density at dendrite tip to the current density of the flat electrode. That is when this ratio reaches to a predetermined temperature threshold, the dendrite growth will transit from the stage of suppressed growth to the stage of uncontrolled dendritic growth. In a temperature range of −25 °C to 25 °C, the author examined his model with the parameters of electrolyte EC:DMC with $LiPF_6$. The model is a function of current density ranging from 2 to 22 mA/cm^2, and the critical temperature gradually increases when the current density increasing.

The effect of current density on dendrite growth rate, was studied in the electrolyte of PC:DMC with 1 M $LiPF_6$ by Akolkar [14], who found that the dendrite growth rate can be

estimated by the local current density at the dendrite tip which is a function of flat surface current density and tip radius. Orsini *et al.* [22] conducted dendrite growth tests on three different types of electrode: lithium, copper, and graphite, under galvanostatic condition up to 2.6 mA/cm^2: 0.22, 0.45, and 0.9 mA/cm^2 for lithium; 0.45 and 2.6 mA/cm^2 for copper; less than 0.1 mA/cm^2 for graphite (exact value not reported). Among their test results, increasing of current density leads to the lithium dendrite morphology from ''moss'' (mossy) to ''bulge'' (shaper than mossy, but not dendritic) to ''dendrite'' (dendritic). Seong *et al.* [15] employed the ''total amount of discharge'' (discharge coulombs) as an indicator to quantify the current density effect on the lithium powder electrode. The electrolyte of EC:DMC with 1 M $LiClO_4$ were used and samples were tested under galvanostatic condition at 0.2, 0.5, 1, 2, and 5 mA/cm^2. Brissot *et al.* [8] studied the dendrite growth in symmetric lithium cells at 80 °C in the polymer electrolyte which is the combination of poly(ethylene oxide) and $LiN(CF_3SO_2)_2$. Samples were tested under galvanostatic condition at 0.03, 0.05, 0.1, and 0.7 mA/cm^2. According to the difference of the dendrite growth onset time, current densities were classified into two regions (separated at 0.18 mA/cm^2) where the formed dendrites have different morphologies.

To observe the dendrite behavior, techniques such as scanning electron microscopy (SEM) [22] and nuclear magnetic resonance (NMR) [23] have been employed. However, these methods are not able to provide the in-situ monitoring to establish the relationship between dendrite growth and electrical signals. Aryanfar *et al.* [24] developed a cylindrical-shaped optical sample to study ''dead lithium'' formation in the cycling process, but this type of cylindrical observation window causes image distortion and requires image pretreatment. Steiger *et al.* [25] constructed a micrometer-level optical sample to observe the behavior of a single dendrite in the cycling process. The dendrite growth direction captured in their work was attributed to the change in the growth point among the dendrite tip, bottom, and kink. However, the theory may not be suitable to explain the dendrite growth direction change in millimeter scale. Love *et al.* [11] implemented a dendrite observation using an optically transparent cell, which will avoid the weakness of the design in [24] and [25]. Our work follows the work of Love *et al.* with some improvements. In addition, we use the cell fixture to study additional cell parameters leading to dendrite growth.

Current theory about lithium dendrite formation regarded this phenomenon as a direct result of nonuniform current distribution on the electrode. However, the understanding of the dynamics of dendrite formation is still lacking. For instance, there is a debate about the reason the dendrite growth direction changes in the charging process. Nishida *et al.* [18] attributed this phenomenon to the accumulated residual stress in the dendrite growth process, whereas Steiger *et al.* [25] regarded the dendrite growth point change as the reason. As noted, the previous work on dendrites growth involved electrolyte optimization as well as study on the temperature and current effects. The applied current densities are less than 3 mA/cm^2. However, in practice, the localized current density on the dendrite tip can reach up to 100 mA/cm^2 [14]. In order to evaluate dendrite growth mechanisms within a broader range of current density higher current than the existing studies should be included.

In this work, an optically transparent battery cell was developed for in-situ observation of dendrite growth. The experimental setup, materials, and the in-situ observation equipment are introduced in Section 2. The dendrite images collected under different current densities and the corresponding current and voltage data are presented in Section 3. Test results are analyzed and discussed in Section 4, followed by conclusions in Section 5.

II. EXPERIMENTAL SETUP AND TEST PARAMETERS

An optical cell was developed in which we placed a symmetric lithium cell consisting of two lithium electrodes and a liquid electrolyte. The electrolyte was composed of 1 M $LiPF_6$ in EC:DMC (1:1 v/v). The lithium electrodes (Fig. 1) were sandwiched between two transparent quartz windows. Only the rectangular cross-section of the electrode was exposed to the electrolyte, which is the reaction area of the cell. Once the current was applied, the lithium ions generated at the positive electrode will be reduced at the negative electrode. This process represents the dendrite growth in a battery. All the test samples were assembled in a glovebox.

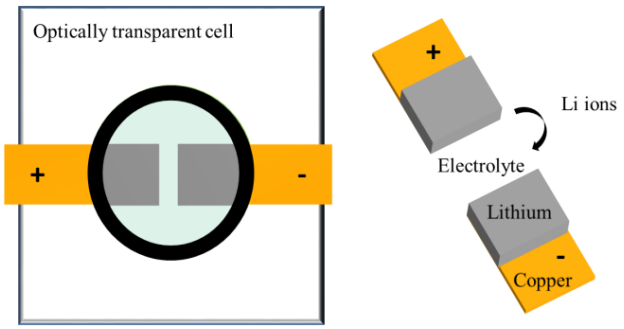

FIGURE 1. Schematic illustration of an optically transparent cell.

Galvanostatic tests were conducted under an ambient condition (around 25 °C) at current densities ranging from 10 to 125 mA/cm^2, using an Arbin BT 2000 battery tester. The selected current density range covered most of the possible lithium dendrite growth scenarios. The current densities were calculated based on the applied current and the electrode cross-section area. The optical images were collected using a digital microscope, and voltage/current signals were continuously recorded. ImageJ software was used to analyze the optical images and to measure the length changes of the lithium dendrites.

III. EXPERIMENTAL RESULTS

Fig. 2 shows the dendrite that formed on the upper part of the negative electrode when the initial average current density

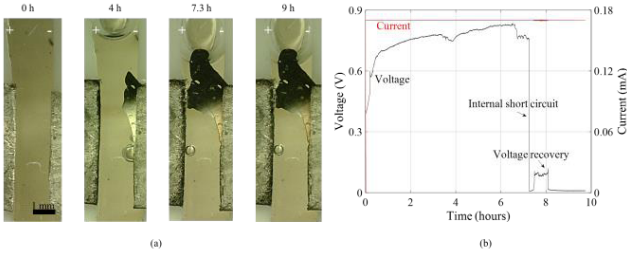

FIGURE 2. The evolution of the dendrite and the electrical signals at a current density of 10 mA/cm^2, (a) the optical images; (b) the corresponding voltage and current profile.

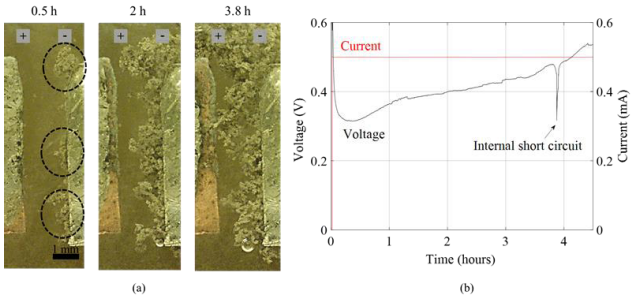

FIGURE 3. The evolution of the dendrite and the electrical signals at a current density of 40 mA/cm^2, (a) the optical images; (b) the corresponding voltage and current profile.

was 10 mA/cm^2. The local electrical field is likely to bias the lithium dendrite initiation position, and in this case, a right-angle corner is a preferential spot due to its higher electric field intensity. The electric field was concentrated around the dendrite tips because of their higher aspect ratio. The first formed lithium dendrite changed the geometry and the electrical field distribution of the negative electrode. Thus, the dendrite tips have higher electrical field intensity than the rest of the flat electrode, and dendrite growth was enhanced at the preferential spot in the following charging process.

The sharp voltage drop at 7.3 h in Fig. 2 indicates an internal short circuit. At the same time, the grown dendrite filled the gap between the positive and negative electrodes and connected them. The voltage recovered 0.3 h later to 0.1 V. A similar voltage recovery phenomenon was reported by Dollé *et al.* [26]. They observed a burnt mark in their sample in which the voltage recovery was attributed to the current-caused dendrite tip damage. In this theory, the dendrite connecting two electrodes was regarded as a fuse. Once the two electrodes were connected, the current could go through the connecting point and cause a temperature rise that breaks the connection. The voltage recovery lasted about 1 h. However, under the constant current charging condition, the lithium dendrite kept growing toward the positive electrode and connected two electrodes again at 8.1 h, which made the voltage drop to zero. As shown by the dendrite images at 7.3 h and 9 h, the shape of the formed dendrite did not change for about 2 h. The dendrite growth stopped after the internal short circuit. The solid connection between the two electrodes was established, and the voltage remained stable after the second voltage drop (at 8.1 h).

The lithium dendrite grew in the transverse direction as well as toward the positive electrode when the applied current density was 40 mA/cm^2. As shown in Fig. 3, at 0.5 h, dendrites initiated mainly at three different spots (circled in Fig. 3(a)) along the edge of the negative electrode. There was no significant dendrite growth between two adjacent spots. After 2 h, lithium dendrites spread along the edge of the negative electrode, and the lithium dendrites at the initiation spots are longer. An internal short occurred at 3.8 h with a voltage drop, however, the voltage did not drop to zero. This phenomenon is called a "soft internal short" because the dendrite structure at such a high current density appears to be a cluster of big lithium particles, and loosely structured lithium dendrites are fragile and easy to break. Thus, in this situation, the voltage recovery may be a result of mechanical stress as well as the above-mentioned heating effect.

Fig. 4 shows dendrite growth at 87 mA/cm^2. The dendrites initiated at the electrode corners are similar to the tests at 10 mA/cm^2. After 1 h, the dendrites gradually extended to the middle part of the electrode. Based on continuous observation, the dendrites in the middle are the extension of the dendrites initiated at the corners. However, the growth rate of the dendrites in the middle is lower than those at the corners. Although it seems the dendrite already connected the two electrodes at 1 h, the corresponding voltage data in Fig. 4 shows the voltage drop occurred at 2.1 h. This time variation is due to the fact that the dendrites did not grow in the same plane. It is possible that the positive electrode and the dendrite tips in the image at 1 h were located in two different planes and seemed overlapped when the image was taken. The real connection was built up at 2.1 h and caused the internal short circuit before the electrode connection, the voltage was stabilized around 0.6 V from 0.5 to 2.1 h as shown in the voltage curve. At 2.1 h, due to the dendrite-caused internal short circuit, the current carrier changed from ions in the electrolyte to the electrons in the metallic dendrite structure. The resistance of metal is much lower than the conductive electrolyte, and the switching caused the voltage to drop sharply. If only the cell voltage is monitored but the dendrite images are not available, there will be no significant

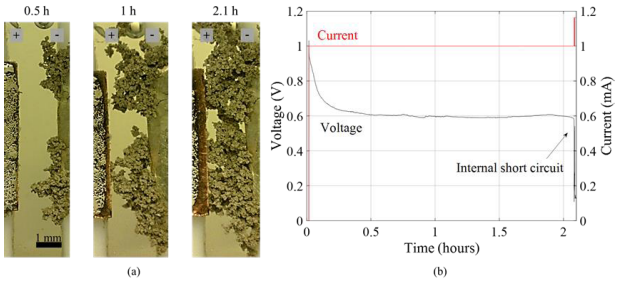

FIGURE 4. The evolution of the dendrite and the electrical signals at a current density of 87 mA/cm^2, (a) the optical images; (b) the corresponding voltage and current profile.

sign of dendrite growth until the sharp voltage drop in the voltage data.

Fig. 5 shows the dendrite growth at 95 mA/cm^2. At 0.5 h, the initial dendrites formed and covered the electrode edge as shown in Fig. 5(a). In this test, the initial dendrites along the edge were not formed at the same time. The initial lithium dendrite had a slightly different length due to the growth time variation. The dendrites initiated earlier are longer and have a higher aspect ratio than the rest. As mentioned in the previous tests, these longer dendrites were the favorable growth spots in the following charging process because the electrical field intensity was higher around them. The earlier growth retained the geometrical advantage. At 1.5 h, several needle-like dendrites presented and grew faster than the other flatly deposited lithium. This result is consistent with Brissot *et al.*'s paper [8] where the formed lithium dendrite grew at several points and has needle-like morphology. These needle-like dendrites led to the first internal shorts. The voltage curve had a drop at 1.5 h, indicating the occurrence of internal short circuit. At 1.5 h, there was a transient increase in the current data. This phenomenon further validates our understanding of the soft internal shorts, which usually do not last long. Therefore, although the voltage recovered, the first voltage drop should be regarded as a warning sign of internal short circuit.

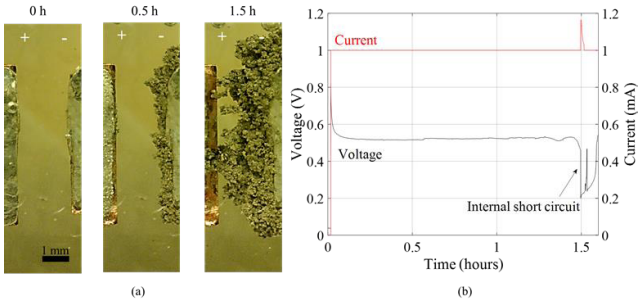

FIGURE 5. The evolution of the dendrite and the electrical signals at a current density of 95 mA/cm^2, (a) the optical images; (b) the corresponding voltage and current profile.

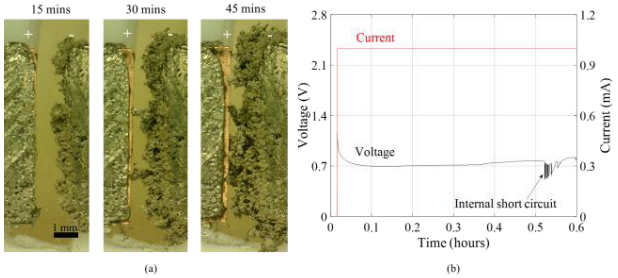

FIGURE 6. The evolution of the dendrite and the electrical signals at a current density of 110 mA/cm^2, (a) the optical images; (b) the corresponding voltage and current profile.

In Fig. 6, the dendrites changed from the mossy growth into the needle-like form when the cell was charged at 110 mA/cm^2. Initially, the dendrite was deposited all along the electrode edge. At around 30 min, there were two needle-like dendrites that connected the two electrodes, which was confirmed from the voltage curve. The formation of the needle-like structures hastened the internal short circuit process.

Test observations conducted at 125 mA/cm^2 are shown in Fig. 7. The dendrite initiated at the electrode corners and the middle, which indicates the electrical field intensity at the middle part of the electrode is now comparable with that at the electrode corner. Also, the electrode geometry influence is weaker than the previous tests. The cell voltage kept increasing from the start of the test, which is due to the cell polarization. Charging at 125 mA/cm^2, the ion movement in the electrolyte reaches its maximum limitation but the mass transfer in the electrolyte is lower than the charge transfer on the electrode. In other words, the mass transfer step is now the controlling step and limits the total reaction speed. The accumulated charges on the electrodes prevented the voltage from stabilizing around a certain value but increased, which was different from the voltage data in previous tests.

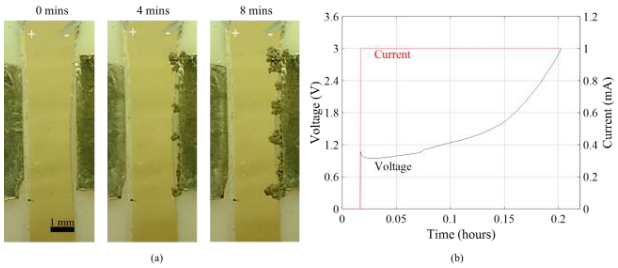

FIGURE 7. The evolution of the dendrite and the electrical signals at a current density of 125 mA/cm^2, (a) the optical images; (b) the corresponding voltage and current profile.

IV. ANALYSIS OF DENDRITE GROWTH AT VARIOUS CURRENT DENSITIES

The growth rate of the dendrites under different current densities was calculated by dividing the dendrite length by the elapsed time until the first voltage drop to evaluate the average dendrite growth rate under certain current densities (see Table 1). In Table 1, the initial current density is the average current density calculated at the beginning of the test.

TABLE 1. Time to the first voltage drop and growth rate.

Initial current density (mA/cm^2)	Time to half of the gap (h)	Time to first voltage drop (h)	Growth rate (mm/h)	Cell voltage (V)
10	3.7	7.3	0.23	0.8
40	0.45	3.88	0.43	0.3
87	0.35	2.08	0.92	0.6
95	0.53	1.48	1.7	0.5
110	0.23	0.5	2.18	0.7
125	N/A	N/A	4.96	1.0

The linear sweep voltammetry (LSV) test determined the current densities range and especially the limiting current density in the EC:DMC (1 M $LiPF_6$) electrolyte. The Tafel lines obtained from the LSV test are shown in Fig. 8 and reflect the relationship between overpotential and current density. The Tafel line gradually turns to parallel with the x-axis at about 100 mA/cm^2. Once beyond the limiting current density, higher current density will not increase the dendrite growth reaction but only the voltage. The increasing tendency of the voltage data shown in Fig. 7 proved this finding and indicates 125 mA/cm^2 is already beyond the limiting current density. In that test, the voltage increased higher than the upper limit (3.0 V) after only 12 min, and the test was stopped. In consideration of the LSV test result and the 125 mA/cm^2 test result, one reasonable estimation of the limiting current density for EC:DMC 1 M $LiPF_6$ electrolyte is in the range of 100 to 125 mA/cm^2.

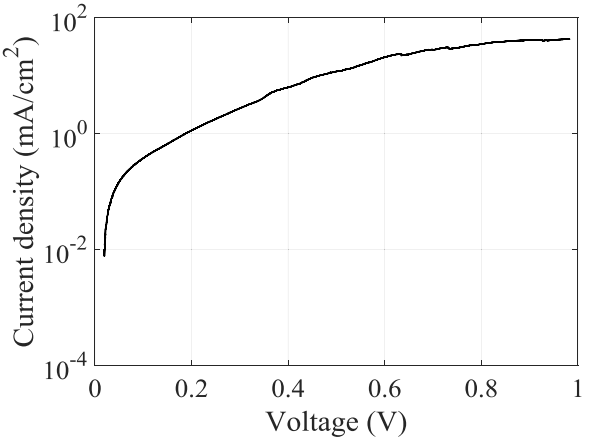

FIGURE 8. Tafel lines of lithium redox to determine the relationship between the overpotential and current density.

During the constant current charging process, both the real-time dendrite images and the corresponding electrical signals were collected until an internal short circuit occurred. The sharp voltage drop indicated an internal short circuit, which was cross-checked with the dendrite images. The time to the first voltage was considered as the elapsed time before the internal short circuit. The corresponding growth rate was calculated based on the length change of the formed dendrites.

The dendrites that grew under different current densities have different growth rates and morphologies. The time when the dendrite length was equivalent to half of the gap between the two electrodes are summarized in Table 1. Based on the time to half of the gap, the estimated times to the first voltage drop are compared with the actual times to the first voltage drop. The results are plotted in Fig. 9. At 10 and 100 mA/cm^2, the estimated values match the actual ones. However, in the middle part, the estimated times are faster than the actual ones owing to the different growth processes. At 10 and 110 mA/cm^2, the dendrites grew in the same morphology from the start of the test until the end. They all grew directly toward the positive electrode. However, when the current

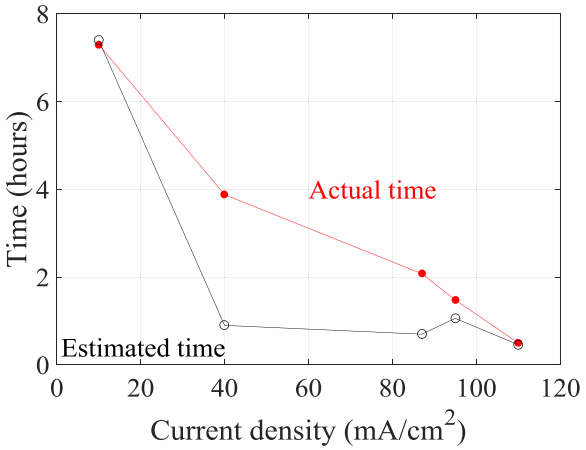

FIGURE 9. Comparison between the estimated time and the actual time to the first voltage drop.

density was in the middle range, they grew in the transverse direction.

The growth rates are plotted against the current densities in Fig. 10. As expected, with the increase in current density, the time to the first voltage drop decreases. The internal short circuit process is hastened with the increased current densities, which is due to the dendrite morphologies change. The needle-like structures shown at higher current densities have a higher aspect ratio than the mossy dendrite and can connect the two electrodes in a shorter time.

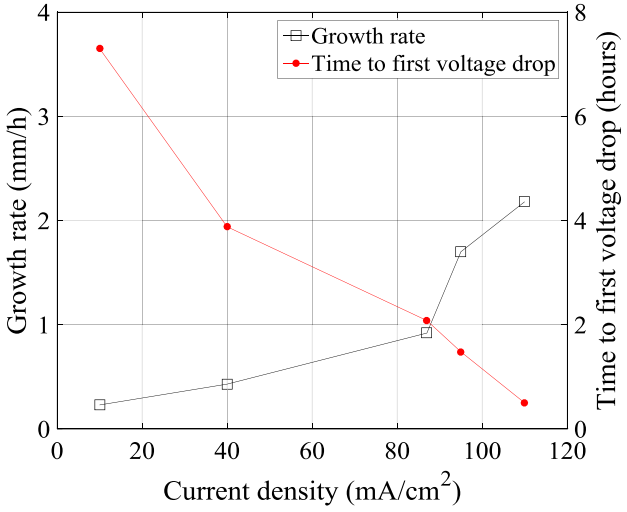

FIGURE 10. Time to first voltage drop and growth rate under various current densities.

After 95 mA/cm^2, the dendrite growth rate is not only higher than the previous test results, but also the curve slope is also steeper. This is due to the change in dendrite morphologies as previously discussed. Previously, the dendrites initiated at the corners of the negative electrode and extended in the transverse direction as well as grew toward the positive electrode. However, with the increase in current density, the dendrite that initiated along the electrode edge and gradually switched to needle-like structure grew toward

the positive electrode directly. In the test at 125 mA/cm^2, the initiated dendrite was already in the needle-like form.

V. CONCLUSIONS

Lithium dendrites are a potential root cause of battery short circuits, thermal runaway, fires, and explosions. However, the inability to observe lithium dendrite growth processes makes it difficult to study the growth mechanisms. This paper developed an optical test fixture which was used to assess dendrite growth behavior under room temperature conditions for current densities in the range of 10 to 125 mA/cm^2.

This approach resulted in the following observations: the average dendrite growth rate increased with the increasing current density; when the current density increased above 87 mA/cm^2, the dendrite morphology changed from flat mossy to sharp needle-like in the growth process; and the initial formation of dendrites changed the electrode geometry and enhanced the electrical field intensity near the tip, which makes this area a preferential growth spot in the following charging process. Controlling the current density is an applicable way to modify lithium dendrite morphology. The observed mossy dendrite is consistent with other works. The needle-like dendrite reported in this work is defined at a millimeter scale, which may not have the same meaning as other dendrites defined at a micrometer level. The smooth and dense lithium dendrite formed at 10 mA/cm^2 is worth further investigation to reveal its growth mechanism.

ACKNOWLEDGMENTS

The authors acknowledge the very helpful assistance of Dr. C. Love at the U.S. Naval Research Laboratory. They also appreciate the more than 150 companies and organizations.

REFERENCES

[1] J.-M. Tarascon and M. Armand, "Issues and challenges facing rechargeable lithium batteries," *Nature*, vol. 414, no. 6861, pp. 359–367, 2001.
[2] Z. Li, J. Huang, B. Y. Liaw, V. Metzler, and J. Zhang, "A review of lithium deposition in lithium-ion and lithium metal secondary batteries," *J. Power Sources*, vol. 254, pp. 168–182, May 2014.
[3] K. Amine *et al.*, "Nanostructured anode material for high-power battery system in electric vehicles," *Adv. Mater.*, vol. 22, no. 28, pp. 3052–3057, 2010.
[4] N. Williard, W. He, C. Hendricks, and M. Pecht, "Lessons learned from the 787 Dreamliner issue on lithium-ion battery reliability," *Energies*, vol. 6, no. 9, pp. 4682–4695, 2013.
[5] D. Djian, F. Alloin, S. Martinet, H. Lignier, and J. Y. Sanchez, "Lithium-ion batteries with high charge rate capacity: Influence of the porous separator," *J. Power Sources*, vol. 172, no. 1, pp. 416–421, 2007.
[6] S.-P. Kim, A. C. T. van Duin, and V. B. Shenoy, "Effect of electrolytes on the structure and evolution of the solid electrolyte interphase (SEI) in Li-ion batteries: A molecular dynamics study," *J. Power Sources*, vol. 196, no. 20, pp. 8590–8597, 2011.
[7] S.-K. Jeong *et al.*, "Suppression of dendritic lithium formation by using concentrated electrolyte solutions," *Electrochem. Commun.*, vol. 10, no. 4, pp. 635–638, 2008.
[8] C. Brissot, M. Rosso, J.-N. Chazalviel, and S. Lascaud, "Dendritic growth mechanisms in lithium/polymer cells," *J. Power Sources*, vols. 81–82, pp. 925–929, Sep. 1999.
[9] N. Schweikert *et al.*, "Suppressed lithium dendrite growth in lithium batteries using ionic liquid electrolytes: Investigation by electrochemical impedance spectroscopy, scanning electron microscopy, and *in situ* ^{7}Li nuclear magnetic resonance spectroscopy," *J. Power Sources*, vol. 228, pp. 237–243, Apr. 2013.
[10] W. Li *et al.*, "The synergetic effect of lithium polysulfide and lithium nitrate to prevent lithium dendrite growth," *Nature Commun.*, vol. 6, Jun. 2015, Art. no. 7436.
[11] C. T. Love, O. A. Baturina, and K. E. Swider-Lyons, "Observation of lithium dendrites at ambient temperature and below," *ECS Electrochem. Lett.*, vol. 4, no. 2, pp. A24–A27, 2015.
[12] R. Akolkar, "Modeling dendrite growth during lithium electrodeposition at sub-ambient temperature," *J. Power Sources*, vol. 246, pp. 84–89, Jan. 2014.
[13] S. Tippmann, D. Walper, L. Balboa, B. Spier, and W. G. Bessler, "Low-temperature charging of lithium-ion cells part I: Electrochemical modeling and experimental investigation of degradation behavior," *J. Power Sources*, vol. 252, pp. 305–316, Apr. 2014.
[14] R. Akolkar, "Mathematical model of the dendritic growth during lithium electrodeposition," *J. Power Sources*, vol. 232, pp. 23–28, Jun. 2013.
[15] I. W. Seong, C. H. Hong, B. K. Kim, and W. Y. Yoon, "The effects of current density and amount of discharge on dendrite formation in the lithium powder anode electrode," *J. Power Sources*, vol. 178, no. 2, pp. 769–773, 2008.
[16] F. Sagane, K.-I. Ikeda, K. Okita, H. Sano, H. Sakaebe, and Y. Iriyama, "Effects of current densities on the lithium plating morphology at a lithium phosphorus oxynitride glass electrolyte/copper thin film interface," *J. Power Sources*, vol. 233, pp. 34–42, Jul. 2013.
[17] D. R. Ely and R. E. García, "Heterogeneous nucleation and growth of lithium electrodeposits on negative electrodes," *J. Electrochem. Soc.*, vol. 160, no. 4, pp. A662–A668, 2013.
[18] T. Nishida, K. Nishikawa, M. Rosso, and Y. Fukunaka, "Optical observation of Li dendrite growth in ionic liquid," *Electrochimica Acta*, vol. 100, pp. 333–341, Jun. 2013.
[19] S. Liu *et al.*, "Effect of co-doping nano-silica filler and N-methyl- N-propylpiperidinium bis(trifluoromethanesulfonyl)imide into polymer electrolyte on Li dendrite formation in Li/poly(ethylene oxide)-Li(CF_3SO_2)$_2$N/Li," *J. Power Sources*, vol. 196, no. 18, pp. 7681–7686, 2011.
[20] R. Mogi, M. Inaba, S.-K. Jeong, Y. Iriyama, T. Abe, and Z. Ogumi, "Effects of some organic additives on lithium deposition in propylene carbonate," *J. Electrochem. Soc.*, vol. 149, no. 12, pp. A1578–A1583, 2002.
[21] A. Aryanfar, D. J. Brooks, A. J. Colussi, B. V. Merinov, W. A. Goddard, III, and M. R. Hoffmann, "Thermal relaxation of lithium dendrites," *Phys. Chem. Chem. Phys.*, vol. 17, no. 12, pp. 8000–8005, 2015.
[22] F. Orsini *et al.*, "*In situ* scanning electron microscopy (SEM) observation of interfaces within plastic lithium batteries," *J. Power Sources*, vol. 76, no. 1, pp. 19–29, 1998.
[23] H. J. Chang *et al.*, "Investigating Li microstructure formation on Li anodes for lithium batteries by *in situ* ^{6}Li/^{7}Li NMR and SEM," *J. Phys. Chem. C*, vol. 119, no. 29, pp. 16443–16451, 2015.
[24] A. Aryanfar, D. J. Brooks, A. J. Colussi, and M. R. Hoffmann, "Quantifying the dependence of dead lithium losses on the cycling period in lithium metal batteries," *Phys. Chem. Chem. Phys.*, vol. 16, no. 45, pp. 24965–24970, 2014.
[25] J. Steiger, D. Kramer, and R. Mönig, "Mechanisms of dendritic growth investigated by *in situ* light microscopy during electrodeposition and dissolution of lithium," *J. Power Sources*, vol. 261, pp. 112–119, Sep. 2014.
[26] M. Dollé, L. Sannier, B. Beaudoin, M. Trentin, and J.-M. Tarascon, "Live scanning electron microscope observations of dendritic growth in lithium/polymer cells," *Electrochem. Solid-State Lett.*, vol. 5, no. 12, pp. A286–A289, 2002.

LINGXI KONG received the B.E. degree in material molding and control engineering from Sichuan University, Sichuan, China, in 2013, and the M.Eng. degree in material science and engineering from the University of Maryland, College Park, MD, USA, in 2015, where he is currently pursuing the Ph.D. degree in mechanical engineering with the Center for Advanced Life Cycle Engineering. His research interests include lithium-ion battery testing and failure analysis of lithium-ion batteries.

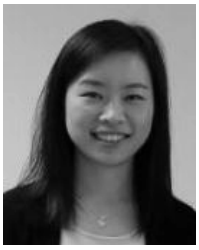

YINJIAO XING received the B.E. degree in mechanical engineering and automation in 2007, the M.E. degree in mechanical and electronic engineering from the Nanjing University of Aeronautics and Astronautics, Nanjing, China, in 2010, and the Ph.D. degree in systems engineering and engineering management from the City University of Hong Kong, Hong Kong, in 2014.

In 2010, she was a Trainee of operation management leadership program with GE Aviation, China. From 2013 to 2014, she was a Senior Research Assistant with the City University of Hong Kong, and a Research Engineer with the Laboratories at HUAWEI Technologies Co. Ltd., China, in 2012. She is currently a Post-Doctoral Associate with the Center for Advanced Life Cycle Engineering, University of Maryland, College Park, MD, USA. Her research focuses on battery system monitoring, modeling, and failure analysis for the purpose of improvement of battery system reliability and operational performance.

She was a recipient of the Highly Cited Applied Energy Award 2015, and one of her first-authored papers has been awarded the Most Cited Microelectronics Reliability Articles published since 2012. She is serving as the Guest Editor of the special issue on Battery Energy Storage and Management Systems in the journal of the IEEE Access.

MICHAEL G. PECHT (S'78–M'83–SM'90–F'92) received the B.S. degree in physics in 1976, the M.S. degree in electrical engineering in 1978, and the M.S. and Ph.D. degrees in engineering mechanics from the University of Wisconsin-Madison, Madison, WI, USA, in 1979 and 1982, respectively.

He is the Founder and Director of the Center for Advanced Life Cycle Engineering, University of Maryland, College Park, MD, USA, which is funded by over 150 of the world's leading electronics companies at more than US6*M*/year. He is also a Chair Professor of mechanical engineering and a Professor of applied mathematics, statistics, and scientific computation with the University of Maryland. He has written over 20 books, 400 technical articles, and has eight patents.

He has also served on three U.S. National Academy of Science studies, two U.S. Congressional investigations in automotive safety, and as an expert to the U.S. Food and Drug Administration. He is a Professional Engineer, a Fellow of the American Society of Mechanical Engineers, a Fellow of the Society of Automotive Engineers, and a Fellow of the International Microelectronics Assembly and Packaging Society. He is the Editor-in-Chief of the IEEE Access, and served as the Chief Editor of the IEEE Transactions on Reliability for nine years and the Chief Editor for *Microelectronics Reliability* for 16 years.